Article

Toward Three-Dimensional Nanoengineering of Heterogeneous Catalysts

Ilke Arslan, John C. Walmsley, Erling Rytter, Edvard Bergene, and Paul A. Midgley

J. Am. Chem. Soc., **2008**, 130 (17), 5716-5719 • DOI: 10.1021/ja710299h • Publication Date (Web): 05 April 2008

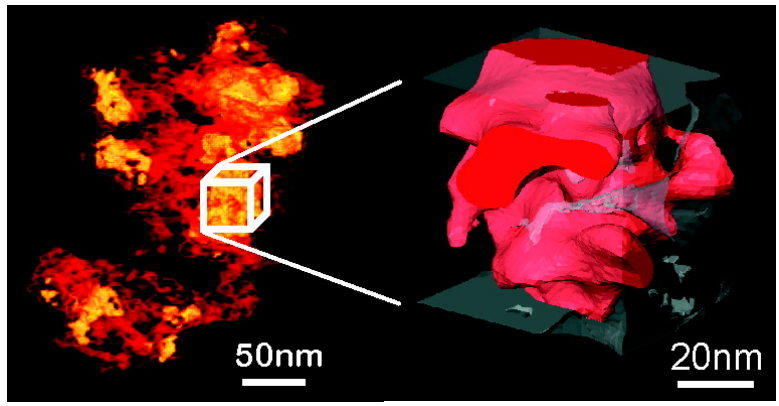

J|A|C|S
ARTICLES

Published on Web 04/05/2008

Toward Three-Dimensional Nanoengineering of Heterogeneous Catalysts

Ilke Arslan,[§,†,*] John C. Walmsley,[‡] Erling Rytter,[⊥] Edvard Bergene,[‡] and Paul A. Midgley[†]

Department of Materials Science and Metallurgy, University of Cambridge, Pembroke Street, Cambridge, CB2 3QZ U.K., SINTEF Materials and Chemistry, Trondheim, N-7465 Norway, and StatoilHydro R&D Research Centre, Postuttak, N-7005 Trondheim, Norway

Received November 20, 2007; E-mail: iarslan@sandia.gov

Ⓦ **This paper contains enhanced objects available on the Internet at http://pubs.acs.org/jacs.**

Abstract: Cobalt-based Fischer–Tropsch systems are widely used to convert synthesis gas to clean hydrocarbon fuel. However, surprisingly little is known about the morphology of the catalysts on the nanoscale. Here we show that scanning transmission electron tomography reveals their true 3-D morphology and provides direct evidence that the support controls the final morphology of the catalyst. Such direct local three-dimensional measurements provide unprecedented insight into catalysis, and can henceforth transform our understanding of these complex materials.

Introduction

The rational design of heterogeneous catalyst systems, typically comprising nanoparticles on a supporting substrate, is paramount to efficient industrial-scale chemical processing. To date, catalyst design has generally relied on the bulk averaged measurement of properties. Future progress will depend increasingly on a molecular scale understanding of systems.[1,2] For example, surface measurements of two-dimensional model systems have been used to gauge a better understanding of the properties of active nanoparticles and their interaction with their support.[3] While some fundamental insights can be made this way, it is vital to bridge the "materials gap" between such model systems and real catalyst systems used in industrial processes.[4–6] One key industrial process, the Fischer–Tropsch (FT) process, has a long history of commercial development and application in conversion of coal, natural gas,[7–9] and (developments toward) biomass[10] to useful, clean hydrocarbon fuel. The importance of FT technology is emphasized by increasing crude oil prices, the need to diversify energy sources with minimum environmental impact and explore sustainable sources. FT catalysts based on cobalt particles on a porous alumina support provide high activity and selectivity to long-chain paraffins, low-water-gas shift activity, and economic viability in converting a variety of hydrocarbon sources to fuel and petrochemical products.[7,9]

To optimize the efficiency of these catalysts and the FT process, a fundamental understanding of the catalysts' size, shape, and distribution, and their relation to catalytic activity/sectivity must be obtained on the nanoscale.[11–16] Standard methods for measuring particle size and dispersion, such as chemisorption and X-ray diffraction (XRD),[17] generate average microscopic properties and give little direct information about the shape and morphology of catalyst nanoparticles particles or their support. In contrast, the transmission electron microscope (TEM) is a powerful tool for the direct study of the size, crystallography, composition, and distribution of catalyst particles.[18,19] While a few conventional TEM studies of cobalt-supported catalyst systems have been reported,[20–22] as cobalt oxide particles are known to aggregate in three-dimensions, a simple two-dimensional TEM image is not sufficient to completely describe their structure.

† University of Cambridge.
‡ SINTEF Materials and Chemistry.
⊥ StatoilHydro Research Centre.
§ Present Address: Sandia National Laboratories, 7011 East Avenue, Livermore, CA 94550.

(1) Bell, A. T. *Science* **2003**, *299*, 1688–1691.
(2) Libuda, J.; Schauermann, S.; Laurin, M.; Schalow, T.; Freund, H. J. *Monatsh. Chem.* **2005**, *136*, 59–75.
(3) Henry, C. R. *Surface Science Reports* **1998**, *31*, 235–325.
(4) St. Clair, T. P.; Goodman, D. W. *Top. Catal.* **2000**, *13*, 5–19.
(5) Goodman, D. W. *Chem. Rev.* **1995**, *95*, 523–536.
(6) Dellwig, T.; Rupprechter, G.; Unterhalt, H.; Freund, H. J. *Phys. Rev. Lett.* **2000**, *85*, 776–779.
(7) Dry, M. E. *Catal. Today* **2002**, *71*, 227–241.
(8) Iglesia, E. *Appl. Catal., A* **1997**, *161*, 59–78.
(9) Schulz, H. *Appl. Catal., A* **1999**, *186*, 3–12.
(10) Tijmensen, M. J. A.; Faaij, A. P. C.; Hamelinck, C. N.; van Hardeveld, M. R. M. *Biomass Bioenergy* **2002**, *23*, 129–152.
(11) Rolison, D. R. *Science* **2003**, *299*, 1698–1701.
(12) Hansen, T. W.; Wagner, J. B.; Hansen, P. L.; Dahl, S.; Topsoe, H.; Jacobsen, C. J. H. *Science* **2001**, *294*, 1508–1510.
(13) Knozinger, H. *Science* **2000**, *287*, 1407–1409.
(14) Reuter, K.; Frenkel, D.; Scheffler, M. *Phys. Rev. Lett.* **2004**, *93*, 116105.
(15) Roeffaers, M. B. J.; Sels, B. F.; Uji-I, H.; De Schryver, F. C.; Jacobs, P. A.; De Vos, D. E.; Hofkens, J. *Nature* **2006**, *439*, 572–575.
(16) Freund, H. J.; Libuda, J.; Baumer, M.; Risse, T.; Carlsson, A. *Chem. Record* **2003**, *3*, 181–200.
(17) Bowker, M. *The Basis and Applications of Heterogeneous Catalysis*; Oxford University Press: New York, 1998.
(18) Gai, P. L.; Boyes, E. D. *Electron Microscopy in Heterogeneous Catalysts*; IOP Publishing, Ltd.: Bristol, 2003.
(19) Thomas, J. M.; Gai, P. L. *Adv. Catal.* **2004**, *48*, 171–227.
(20) Voss, A.; Borgmann, D.; Wedler, G. *J. Catal.* **2002**, *212*, 10–21.
(21) Jablonski, J. M.; Okal, J.; Potoczna-Petru, D.; Krajczyk, L. *J. Catal.* **2003**, *220*, 146–160.
(22) Storsæter, S.; Tøtdal, B.; Walmsley, J. C.; Tanem, B. S.; Holmen, A. *J. Catal.* **2005**, *236*, 139–152.

10.1021/ja710299h CCC: $40.75

Table 1. Important Physical Catalytic Properties for the Two Samples[a]

sample	pore diameter (nm)	total surface area (m^2/g)	porosity	C_5+ selectivity (%)
1	12.2	134.0	0.675	84.7
2	70.0	11.1	0.431	89.5

[a] Sample 1 is 20% Co/0.5% Re on γ-alumina and sample 2 is 12% Co/0.5% Re on α-alumina. Measurements are made by standard techniques.[22,27]

Experimental Methods

Advances in electron tomography[23] in the scanning transmission electron microscope (STEM) now enable reliable and quantifiable three-dimensional reconstructions of inorganic materials to be achieved with a spatial resolution approaching 1 nm in all three spatial dimensions.[24] We apply this technique here to two Re promoted FT catalyst systems[25,26] prepared in the following slightly different ways. The first is a 20 wt % Co/0.5 wt % Re catalyst on a high surface area γ-alumina substrate and the second is a 12 wt % Co/0.5 wt % Re catalyst on a heat-treated substrate of γ-alumina impregnated with 5% Ni. The phases present in the heat-treated support were previously identified by X-ray diffraction as α-alumina (Al_2O_3), and Ni-aluminate ($NiAl_2O_4$). Their catalytic performance and bulk structural properties are summarized in Table 1. Note that the increase in selectivity of the second system ($\sim$5%) appears moderate, but this difference will be of clear significance in a commercial system.

The materials were studied in their unreduced condition so that Co is present in the form of Co_3O_4. Co is the active form for the catalyst and it would have been desirable to study the catalysts in the reduced condition, on which selectivity measurements were made. However, the cobalt nanoparticles in these materials oxidize rapidly on exposure to air, providing an experimental limitation in transferring the sample to the electron microscope without the Co oxidizing. If the samples were in their reduced state, it is expected that the overall morphology and distribution of the Co would remain the same, while small-scale changes associated with the change in structure and volume of the Co component might be expected.

It is known that pore geometry influences catalytic properties,[27] coarser α-alumina supports give increased long-chain hydrocarbon selectivity,[28] and the formation of the aluminate stabilizes the structure of the support. Therefore, two material changes have been carried out between the first and the second catalytic system. First, high temperature calcination transforms γ-alumina to α-alumina, giving a significant increase in selectivity, but at the expense of the material strength, and to some extent, the catalytic activity. Second, by adding a nickel compound before the high-temperature treatment, the now modified catalyst–support becomes extremely strong and most of the lost activity is regained.[29] This nanostructure is associated with superior mechanical properties. However, a nanoscale understanding of why this activity has been regained has not existed until now. In the remainder of this paper we will show how STEM tomography is used to gain this fundamental understanding. Because of the three-dimensional nature of the results, the movies provided as web-enhanced objects are a key component of this paper and should be viewed while studying the figures.

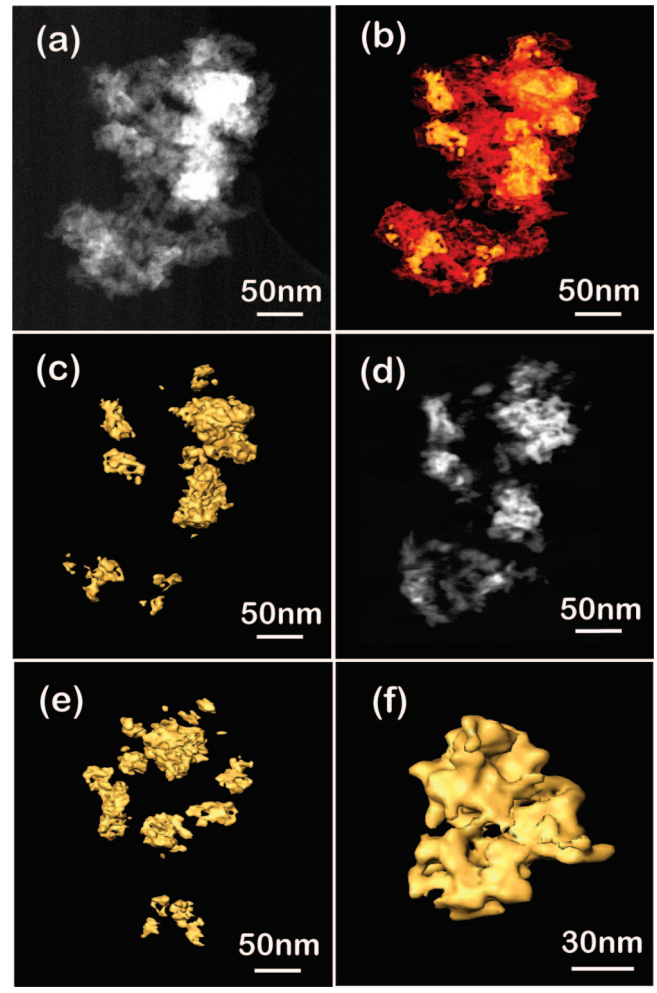

Figure 1. Cobalt oxide catalyst in γ-alumina: (a) a typical STEM HAADF image; (b) a volume-rendered tomographic reconstruction showing the alumina support in red and the cobalt oxide catalyst in yellow. It can be seen that the substrate is highly porous, and the cobalt oxide forms agglomerated clusters; (c) a surface render of the reconstruction showing the morphology of the cobalt oxide. By comparison to panel b, it can be seen that much of the alumina pore space is unfilled and the cobalt oxide itself is porous. This is seen also in the brighter areas of the 1 nm slice of the reconstruction in panel d. Panel e is a surface render of the cobalt oxide at an angle perpendicular to that shown in panel c, and panel f shows a detailed view of one of the cobalt oxide clusters. The cobalt oxide and alumina support form an interlocking structure.

Ⓦ Movie in mpg format of the cobalt oxide/γ-alumina catalyst that demonstrates the interlocking pore structure of the support and the catalyst.

Results and Discussion

Tomography tilt series of 141 images were acquired over the range $-70°$ to $+70°$ for both systems. Results from the Co_3O_4/γ-alumina system are shown in Figure 1 and Movie 1. A typical STEM high angle annular dark field (HAADF) image (Figure 1a) shows how the Co_3O_4 particles appear bright relative to the alumina, but the contrast is complicated by thickness variations and there is limited useful information due to the two-dimensional nature of the image. An enormous increase in information can be gained in three-dimensions, as illustrated in the tomographic reconstruction (Figure 1b). This figure shows the alumina support in red and the Co_3O_4 in yellow and Figure 1c shows only the cobalt oxide. It is immediately evident that

(23) Midgley, P. A.; Weyland, M. *Ultramicroscopy* **2003**, *96*, 413–431.
(24) Arslan, I.; Yates, T. J. V.; Browning, N. D.; Midgley, P. A. *Science* **2005**, *309*, 2195–2198.
(25) Vada, S.; Hoff, A.; Adnanes, E.; Schanke, D.; Holmen, A. *Top. Catal.* **1995**, *2*, 155–162.
(26) Iglesia, E.; Soled, S. L.; Fiato, R. A.; Via, G. H. *J. Catal.* **1993**, *143*, 345–368.
(27) Borg, Ø.; Storsaeter, S.; Eri, S.; Wigum, H.; Rytter, E.; Holmen, A. *Catal. Lett.* **2006**, *107*, 95–102.
(28) Schanke, D.; Eri, S.; Rytter, E.; Aaserud, C.; Hilmen, A. M.; Lindvag, O. A.; Bergene, E.; Holmen, A. *Stud. Surf. Sci. Catal.* **2004**, *147*, 301–306.
(29) Rytter, E.; Skagseth, T. H.; Wigum, H.; Sincadu, N. GB0401829.7, WO 2005/072866 A1, 2004.

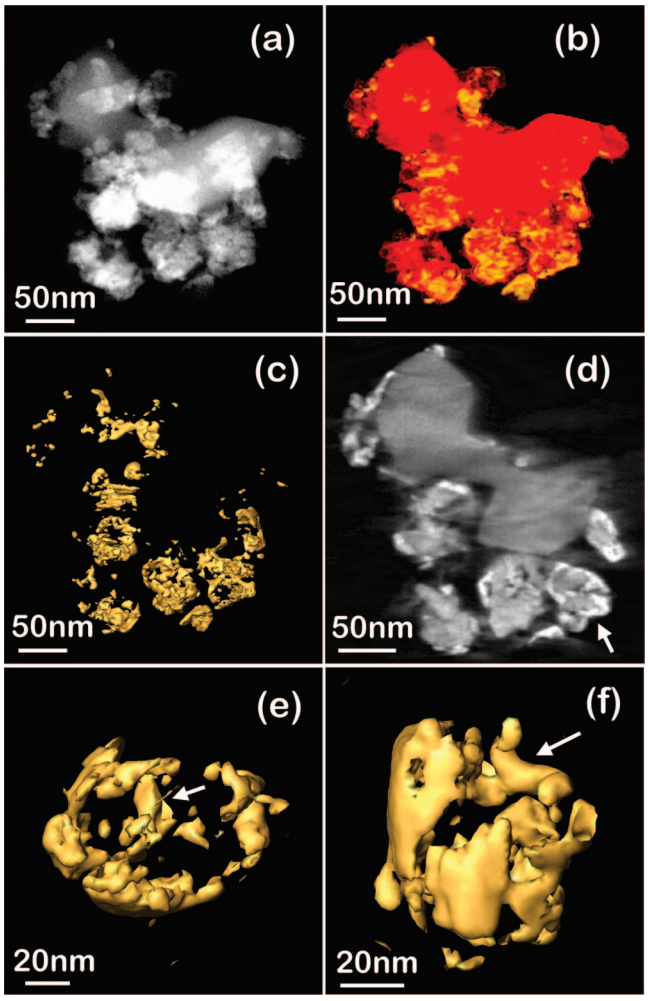

Figure 2. Cobalt oxide catalyst in α-alumina/Ni-aluminate: (a) a typical STEM HAADF image; (b) a volume-rendered tomographic reconstruction showing the alumina support in red and the cobalt oxide catalyst in yellow. The α-alumina is composed predominantly of large nonporous particles. The smaller more porous particles towards the bottom are Ni-aluminate; (c) a surface render of the reconstruction showing only the cobalt oxide. The cobalt oxide does not penetrate the substrate, but wets the surface of the support. For the smaller Ni-aluminate particles, the cobalt oxide forms into cage-like structures; (d) a 1 nm slice through the reconstruction showing that the cobalt oxide (brighter areas) wets the surface of the substrate, most clearly seen at the bottom right (indicated by the arrow). Panels e and f are surface renders of the single cluster arrowed in panel d; the morphology of the cobalt oxide "cage" is clear. Examination of the reconstruction shows that just one of the Ni-aluminate pores is partially filled by the oxide, indicated by an arrow in both panels e and f.

Ⓦ Movie in mpg format of the cobalt oxide/α-alumina/Ni-aluminate catalyst.

the alumina is very porous, and that in fact the catalyst agglomerates are highly porous as well. A 1 nm thick slice through the reconstruction (Figure 1d) actually illustrates that the Co_3O_4 (brighter areas) fills the alumina pores, forming interlocking oxide/support clusters. The classic model of cylindrical pores with the catalytic component attached to the walls evidently is not valid here. Figure 1e highlights the pore-filling distribution of the Co_3O_4 agglomerates and Figure 1f illustrates the porosity of single agglomerate in detail. Before we discuss one of these agglomerates in more detail, we present an overview of the second catalyst system.

Figure 2 and Movie 2 display the results from the Co_3O_4/Ni-aluminate/α-alumina system. A typical STEM HAADF image (Figure 2a) illustrates that the support is coarser than the first sample, but again a more detailed understanding cannot be obtained from this 2-D image. Figure 2b is a three-dimensional reconstruction with the support in red and the Co_3O_4 in yellow. The large solid-red areas are α-alumina, whereas the smaller red clusters in proximity to the cobalt oxide (yellow) represent the nickel aluminate. Figure 2c shows strikingly that the Co_3O_4 encloses the finer component of the support, that is, the Ni-aluminate. A 1 nm thick slice through the reconstruction (Figure 2d) shows that the metal oxide (brighter areas) appears to "wet" the support, forming a shell-like structure around the support in this 2-D image, indicated by an arrow. Figure 2 panels e and f are high resolution reconstructions of this Co_3O_4 "nanocage" structure around the support, with only one pore partially filled, indicated by an arrow. A separate TEM examination of the substrate material confirmed that the microstructure comprises a fine distribution of Ni-aluminate within a coarse α-alumina skeleton. This is consistent with the contrast seen in Figure 2d, in which the Ni-aluminate shows slightly stronger contrast than the α-alumina because of its higher average atomic number. Importantly, very little cobalt is associated with α-alumina and a clear preference is shown by the catalyst to form nanocages around the Ni-aluminate substructure.

To study both of these catalyst systems in more detail, segmentation can be performed on a small region of choice of the larger volume reconstruction. Segmentation of a reconstruction allows for the surface area and volume to be measured, and a porosity and pore size to be calculated from these values locally for the cobalt oxide and substrate. Segmentation works best for systems, such as these, in which the phases (here the metal oxide and support) have a large difference in contrast in the images. Figure 3a–c and Movie 3 show the results from the first sample (a Co_3O_4 on γ-alumina cluster), and Figure 3d–f and Movie 4 show results from the second (a Co_3O_4 on Ni-aluminate cluster). In Figure 3a, a $(40\ nm)^3$ volume of the Co_3O_4/γ-alumina system reveals in detail the interlocking porous structure: the gray semitransparent material is the γ-alumina, and the red is the Co_3O_4. The only open pore of the γ-alumina in the volume can be seen to propagate from the front right side to the front left side of the volume of data. Figure 3b shows only the γ-alumina, and by comparison with Figure 3a, it can be seen that all but one of the pores are filled with cobalt oxide. Figure 3c shows one of the apparently highly porous Co_3O_4 agglomerates. The porosity of the γ-alumina volume is measured to be $73\% \pm 5\%$, and the Co_3O_4 is $77\% \pm 5\%$, which is in reasonable agreement with the bulk nitrogen physisorption value of 67% in Table 1. Within experimental error, the porosities of the two are equal, indicating their intimate connectivity. For this system, the average pore size in the analyzed volume is estimated to be 14 nm, which is in good agreement with the value of 12.2 nm from bulk measurements given in Table 1. The strength of nanoscale tomographic analysis, however, lies in the ability to interpret such measurements with a far greater knowledge of the catalysts' fine-scale three-dimensional architecture.

Figure 3d shows a $(60\ nm)^3$ volume of the Co_3O_4/Ni-aluminate/α-alumina system highlighting the coating of a Ni-aluminate cluster and the distribution of the cobalt oxide in the support. Figure 3e confirms the Ni-aluminate is highly porous, but despite this, as seen in Figure 3f, the cobalt oxide lies predominantly on the surface. A porosity value cannot easily be defined for this cage-like morphology. However, a specific surface area (with respect to its mass plus that of the nickel aluminate) of $64 \pm 5\ m^2/g$ can be measured within this volume. This local value is far higher than the bulk value of $11.1\ m^2/g$ given in Table 1 because the α-alumina is excluded (the α-alumina itself was too coarse relative to the size of the

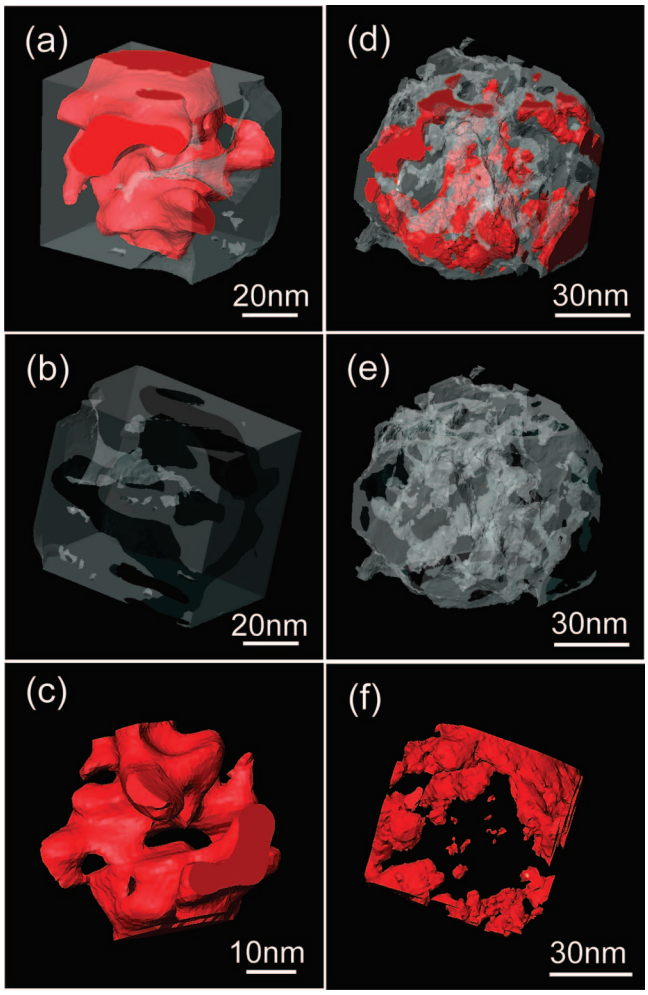

Figure 3. Segmentation of the two systems: (a–c) the Co_3O_4/γ-alumina system and (d−f) the Co_3O_4/Ni-aluminate/α-alumina system. The color scheme was necessarily changed from the previous figures to show the detail in the segmented regions more clearly: (a) the Co_3O_4 in red and the γ-alumina in semitransparent grey; (b) only the alumina, rotated 180° with respect to panel a. The darker grey areas indicate the porous regions in which the cobalt oxide resides; (c) agglomerates of the cobalt oxide particles are also very porous; (d) Co_3O_4 in red on a Ni-aluminate cluster in semitransparent grey; (e) only the highly porous Ni-aluminate; and (f) despite the porosity, the cobalt oxide chooses to stay primarily on the surface and form "nanocages."

Ⓜ Movie in mpg format of a small segmented area of the cobalt oxide/γ-alumina catalyst showing more clearly the interlocking structure.

Ⓜ Movie in mpg format of a small segmented area of the cobalt oxide/α-alumina/Ni-aluminate catalyst.

reconstructed volume to allow a measurement to be made). The porosity of the Ni-aluminate in the volume was measured to be 57% ± 5%, and the bulk measurements for this catalyst yield an overall porosity of 42%. The calculated pore size for the Ni-aluminate is ∼20 nm. This cannot be compared to the bulk measurements because the porosity of the Ni-aluminate is only one small part of the larger system. The bulk measurements are clearly insensitive to the structural complexity of the system. In both systems, the porosity values measured using tomography yield higher values than those measured by nitrogen physisorption. This is because the STEM tomography technique gives quantitative nanoscale information at the site of the activity as opposed to randomly in the bulk, which is much more accurate locally since the clusters where activity occurs are not necessarily representative of the bulk structure overall.

It is curious that the Co_3O_4 in the second system preferentially precipitates on the nickel aluminate and not the α-alumina, and that it forms nanocages on the surface rather than sitting inside the pores (like the first system). We believe this happens for two reasons: first the nickel-aluminate forms small imperfect crystals that provide a high surface area for precipitation, and second, its spinel structure contains vacant metal sites which may accommodate cobalt atoms, while the α-alumina is very regular in morphology with a chemically inert surface. Since the aluminate forms small clusters, it will be more favorable for the catalyst to cover the surface of the clusters to get the most exposure to the vacant metal sites, rather than moving into the less dense, porous interior. These 3-D reconstructions are the first direct observation of this phenomenon on the nanoscale. This unexpected Co_3O_4 distribution undoubtedly provides a more open local environment for reactions to take place, and we believe that the influence of this nanostructure must be taken into account in understanding the higher C_5+ selectivity relative to sample 1 (Table 1). In future experiments, it will be important to study these systems with the Co component in a reduced state to provide the complete nanoscale picture of the structure and further understand the subtle observed changes in reactivity. In the γ-alumina material, nanoscale changes to the Co_3O_4 are likely to be relevant on the scale of the pores and reactant molecules. In the coarser α-alumina material, the behavior of the relatively large slabs of oxide upon reduction will be important for judging the reactive surface area and nature of catalytic sites.

Conclusions

High resolution STEM tomography of cobalt-based FT catalysts reveals how the three-dimensional size, shape, distribution, and porosity of the catalyst and its support can be determined with great clarity and accuracy and with a spatial resolution approaching 1 nm. This powerful 3-D information gives us direct insight into the nanoscale differences between catalyst systems that are invisible to bulk property measurements. We have shown here that the higher selectivity of one catalyst system over the other correlates with the 3-D nanocage morphology and its selection of the nickel-aluminate support over α-alumina. The less selective catalyst has a morphology of fully interlocking catalyst/support aggregates in the unreduced condition that suggests a low exposed cobalt oxide surface area within the pores. The ability to understand and optimize parameters that influence specific properties, for instance selectivity, is of tremendous potential for the future design of heterogeneous catalysts such as FT systems that play a key role in the management of energy supply for hydrocarbon production with a positive environmental impact.

Acknowledgment. This work was supported by the Royal Society and the National Science Foundation in the form of Fellowships for I.A., and was partially funded by Sandia's President Harry S. Truman Fellowship LDRD. Work at Sandia is supported by the Department of Energy, under contract DE-AC04-94AL85000. J.C.W. acknowledges StatoilHydro ASA for financial support. We thank the Isaac Newton Trust for financial support and P.A.M. acknowledges financial support from the European Union under the Framework 6 program under a contract for an Integrated Infrastructure Initiative, Reference 026019 ESTEEM.

JA710299H